Microscale thermography of freezing biological cells in view of cryopreservation

Christophe Pradere * — Junko Morikawa — Jean Toutain* — Jean-Christophe Batsale* — Eita Hayakawa** — Toshimasa Hashimoto****

** Laboratoire TRansfert Ecoulements FLuides et Energétique (TREFLE), Université Bordeaux 1, UMR CNRS-ENSAM-UB1 8508, Esplanade des Arts et Métiers, 33405 Talence, France*

christophe.pradere@bordeaux.ensam.fr - toutain@enscpb.fr - jean-christophe.batsale@bordeaux.ensam.fr

*** Tokyo Institute of Technology, O-okayama, Meguro-ku, Tokyo 152-8550, Japan.*

morikawa.j.aa@m.titech.ac.jp - ehayakaw@katch.ne.jp hashimoto.t.ae@m.titech.ac.jp

ABSTRACT: *The aim of this work is to present a device for the measurement of biological living tissues during freezing by infrared camera. Under simplified assumptions, it is shown that infrared thermography measurements and two-dimensional microscale thermal processing methods of the temperature frames allow to estimate important thermophysical fields for the cryopreservation of living tissues, such as the heating source distribution of the latent heat released from biological cells and the thermal properties during freezing.*

This work is related to the analysis of thermal source terms occurring during freezing of biological tissues from the processing of experimental temperature fields obtained by infrared thermography. Such information is very important in order to understand and improve the heterogeneous solidification phenomena during cryopreservation processes. A new method is proposed here in order to estimate the 2D mapping of source terms and thermal diffusivity during freezing. Such source terms (space and time distributions) are strongly related to the thermal diffusivity mapping which control the 2D in plane diffusion into the tissue.

KEY WORDS: *Temperature field processing, Phase change estimation, thermophysical properties.*

Received December 19, 2008; Accepted March 11, 2009.

QIRT Journal. Volume 6 – N° 1/2006, pages 37 to 61

1. Introduction

The theory and technique of cryo-preservation of biological cells and whole tissues have been studied for long time (Mazur, 1963; Diller, 1975; Levin, 1981; Toner *et al*., 1990), and the principles of phenomena which can cause damage to cells during preserving process are understood by solution effects, extra cellular ice formation, dehydration, and intracellular ice formation. However, the freezable cells and tissues are still limited and preserving organs for storage and transplant is still on the way.

Although, successful cryopreservation can be achieved for a variety of isolated cells in suspension, attempts to freeze the whole tissues and organs have proved unsuccessful. Current techniques for the preservation of tissues are primarily empirical extensions of protocols developed for cellular systems. Tissues are now routinely cryopreserved, and some improvements are required to meet increasing clinical demands.

Tissues are a complex system of organized cells that maintain their structure and function through the development of cell junctions. Cell interactions have been identified as important determinants for the tissue response in cryopreservation, which appears to be sites for tissue damage by the osmotic stresses and phase changes involved in the process of cryopreservation. For example, during cooling the intracellular ice formation occurs when both the cell cytoplasm's super cooling and a nucleation occur, subsequent to the development of the osmotic gradients across the membrane. The membrane is an effective barrier to the propagation of ice but this barrier might be breached for nucleation to occur.

Cryopreserving is a thermal control technique; however, the scientific view has been more concentrated on the medical and cellular pathology. To quantify the cell death has been executed by the typical methods of cellular pathology, by staining cells for the fluorescent microscopy with the result of a biological assay.

Until recently the direct view of latent heat of inter- and intra-cellular ice formation and thermal diffusion over the tissues (Hashimoto *et al.*, 2003; Morikawa *et al*., 2006), had not been performed. It was shown that by using a high-speed IR camera with a micro-scale spatial resolution the latent heat explosion from each cell and the dissipation over the tissues are clearly visualized. This suggests there is a potential to analyze where the ice formation starts, how the heat transfers over the tissues, and how the cell dies in the thermal process. In previous studies (Morikawa *et al*., 2006), the authors tried to estimate the source term distribution with a time derivative of instantaneous temperature field. Nevertheless, such models did not take into account the in-plane thermal diffusion and the heterogeneous nature of the biological tissues.

The present work tries to improve the heat source terms mapping with a 2D-transient simplified heat transfer model and inverse methods.

The main difficulty of such a situation is to estimate simultaneously the local heat diffusion parameters related to the heterogeneous tissue and a source term distribution non-uniform in space and time. The main originality of our method is to estimate the thermal diffusivity field by using the heat dissipated by the heat source generated during the phase change in the onionskin. Then, the estimated thermal diffusivity is taken for an a posteriori calculation of the heat source. The thermal diffusivity field related to the experimental data zone where no source term occurs. is obtained via a calculation of a correlation coefficient between the local temperature Laplacian and time derivative.

In order to show several characteristics and performances of this method, a simple numerical experiment is explained and commented. Then, experimental validation is realised on a thin glass layer and results obtained with onionskin tissues are discussed.

2. Numerical experiment: direct model and inverse processing

2.1. *Direct model*

Onionskin cell was used as a typical plant cellular tissue linked and separated with the cell wall. A thin and translucent piece of tissue was peeled from the inner surface of the second stratum of onion. The averaged cell size is about 80 μm x 200 μm in area size and 80 μm in thickness. The specimen was directly placed on a thin gold plate of 100 μm thickness fixed on a specimen holder settled on the Peltier chip in a vacuum chamber, the temperature of which was reduced in a controlled manner at a constant cooling rate of 80°C/min from room temperature to -20°C. In order to avoid condensation of water on the specimen surface and heat losses, the measurement was conducted under low vacuum conditions. The vessel was filled with dried nitrogen gas. A sapphire glass was used as an observation window. The high-speed IR camera Radiance HS (Raytheon), having an indium-antimony (InSb) sensor array of 256 x 256 pixels with an optimum wavelength between 3 μm and 5 μm was used. The frame rate for taking images was selected at 368 frame/s (2.7 ms per picture) in this study. By using a silicon germanium IR microscopic lens, we could visualize an area of 1.9 mm x 1.9 mm at four times magnification corresponding to a spatial resolution of 7.5 μm x 7.5 μm for each pixel. The absolute temperature of the specimen was calibrated using an ultra-thin K type thermocouple inserted into the specimen. The intensity of radiation detected by the IR FPA camera was converted into 12 bit digital data. After consideration of the relationship between temperature and digital count number, a temperature resolution of 20 mK was obtained. The setup is shown in Figure 1. The temperature field of the glass plate is recorded as a function of time with an infrared camera. Therefore, with this configuration, the general analytical thermal model is:

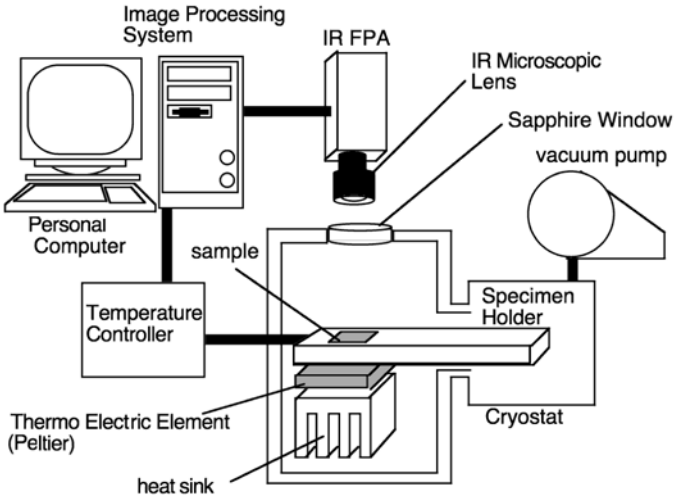

Figure 1. *The experimental setup for freezing of onion skin cells.*

$$\rho C_p \frac{\partial T(x,y,z,t)}{\partial t} = div(\lambda\, grad\left(T(x,y,z,t)\right) + \varphi(x,y,z,t) - h\left(T(x,y,z,t) - T_a\right) \quad [1]$$

As the sample is in a vacuum chamber, we assumed that the thermal heat losses are small. Further, as the thickness of the onion cell is low (< 80 µm), only the 2D heat transfer in plane is considered. Finally, as the area of the onionskin is much larger in comparison with the one of the cell, we supposed the onion as a semi-infinite media in *x* and *y* directions. We also assumed that the thermal conductivities are constants and the same in *x* and *y* directions. With all this assumptions, the thermal problem is rewritten as follow:

$$\rho C_p \frac{\partial T(x,y,t)}{\partial t} = \lambda \Delta T(x,y,t) + \varphi(x_W, y_W, t) \quad [2]$$

with the boundary conditions at:

$$\begin{aligned} &t = 0, \;\; T(x,y,t) = 0 \\ &x = \pm L_x, \frac{\partial T(x,y,t)}{\partial x} = 0 \\ &y = \pm l_y, \frac{\partial T(x,y,t)}{\partial y} = 0 \end{aligned} \quad [3]$$

in addition, the expression for the heat source term:

$$\varphi(x_W, y_W, t) = \varphi_0 \quad for \begin{cases} -L_W < x < L_W \\ -l_W < y < l_W \\ t_0 < t < t_f \end{cases} \qquad [4]$$

with: T temperature (K), ρ mass density (kg m^{-3}), C_p specific heat (J kg^{-1} K^{-1}), λ thermal conductivity (W m^{-1} K^{-1}), x,y space coordinates, L,l length and width of onionskin (m), L_W,l_W length and width of onion cell with water (m), t_0,t_f time window where the heat source is active (s) and $\varphi(x_W, y_W, t)$ local heat source term (W m^{-3}).

In order to solve such system, the 2D finite differences approximation with explicit scheme is performed by considering the temperature signal $T_{i,j}^k$ of one pixel at node i,j and at time k:

$$Fo_{i,j}\Delta T_{i,j}^k + \Phi_{i,j}^k = \delta T_{i,j}^k \qquad [5]$$

with: $\Delta T_{i,j}^k = \left(T_{i+1,j}^k + T_{i-1,j}^k + T_{i,j+1}^k + T_{i,j-1}^k - 4T_{i,j}^k\right)$ and $\delta T_{i,j}^k = T_{i,j}^{k+1} - T_{i,j}^k$ the Laplacian and the temporal derivative of the temperature, $Fo_{i,j} = \dfrac{a_{i,j}\Delta t}{\Delta x^2}$ is the non dimensional Fourier local number with: $a_{i,j}$ the local thermal diffusivity (m² s^{-1}), Δx the pixel size (m) with $\Delta x = \Delta y$, Δt the time step (s) and, $\Phi_{i,j}^k = \dfrac{\varphi_0 \Delta t}{\rho C_p}$ is the heat source in (°C) with: ρC_p (J m^{-3} K^{-1}) the volumic specific heat and φ_0 (W m^{-3}) the volumic heat source.

The model described by the equation [5] is simulated in order to present the inversion processing. For that, the parameters used for the simulation are: the thermal diffusivity a = 10^{-6} m² s^{-1} for all the media, the volumic specific heat ρC_p = 10^6 J m^{-3} K^{-1}, the volumic heat source φ_0 = 1.10^7 W m^{-3}, the pixel size $\Delta x = \Delta y$ = 300 µm, the time step of acquisition Δt = 20 ms, the number of pixels in the x and y directions identical and equal to 64, the number of time step equal to 200, the heat source centred with $l_w = L_w$ = 3 pixels (Figure 2a) and with the function of time of the Figure 2b. Here, the pixels correspond to finite element nodes. This gives theoretical values of 4.5 for the inverse Fourier number (*1/Fo*) and 0.2 for the heat source (Φ).

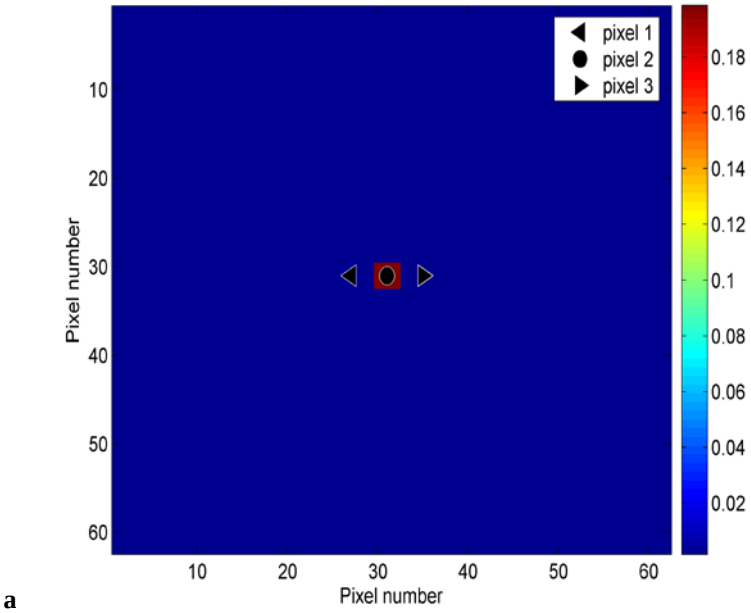

a

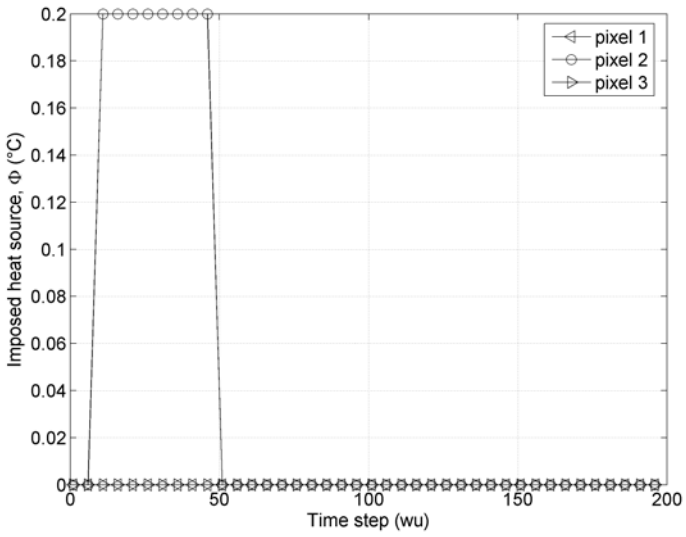

b

Figure 2. *Properties of the heat source:* **a***) spatial location field at time step Δt = 40 and* **b***) temporal evolution for the same three pixels located in the field.*

With these parameters and with the equation [5], we obtained temperature fields at different time steps presented in Figure 3.

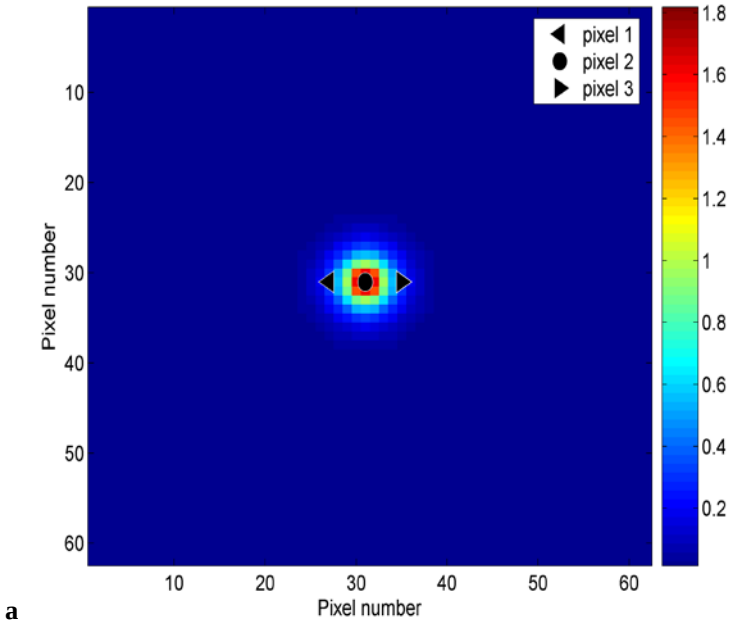

a

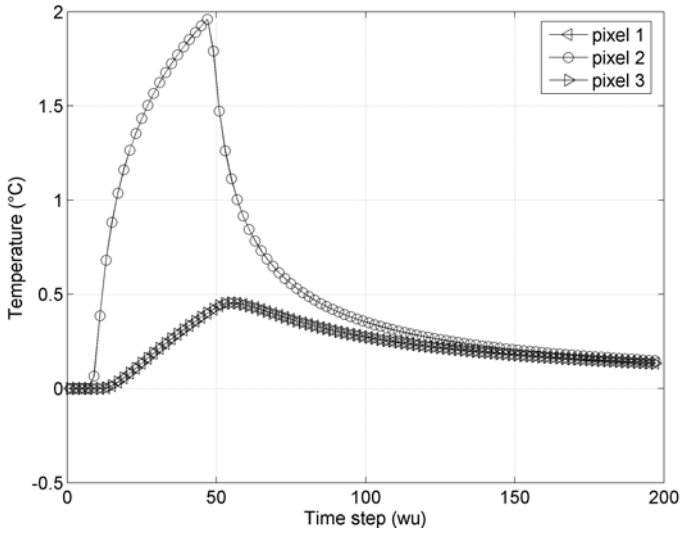

b

Figure 3. *Simulated temperature response:* **a***) spatial field representation at time step* $\Delta t = 40$, **b***) as function of time for the same three pixels located in the field.*

The main difficulty is to perform the processing method with this simple case in order to estimate the fields of thermal diffusivities and source terms.

For the processing, the data (i.e. temperature field) are noised with a white noise similar to the infrared camera Noise Equivalent Temperature Difference (NETD) of (20 mK).

2.2. *Inverse processing*

Even if equation [5] gives theoretically a way to estimate the fields of Fourier and source terms inside the system, the influence of the measurement's noise must be taken into account. Unfortunately, the estimation is only possible if the derivation of the signal does not severely amplify such measurement's noise. In practice, the estimation of $Fo_{i,j}$ is only possible if the quantities $\Delta T_{i,j}^k$ and $\delta T_{i,j}^k$ are not too small.

One of the main characteristic of the previous direct model is that the source term is present only in very small sized location of the image and during a short time. Otherwise, all the temperature data would relax versus the experiment time, satisfying the following relation:

$$Fo_{i,j}\Delta T_{i,j}^k = \delta T_{i,j}^k \qquad [6]$$

The main difficulty consists in finding in the temperature cube (space and time), the pixels verifying the simple diffusive model [6]. One simple way to process the temperature is, just to plot the Laplacian versus the temporal derivative (Figure 4) for the three pixels located in the field (see Figures 2 or 3).

The results show two linear behaviours, the first one corresponds to the points (i.e. time steps) where the heat source is off (triangles corresponding to pixels 1 and 3 and circle of pixel 2), and the other one to the heat source on (circle of pixel 2). When the heat source is off, the data evolve linearly and passes through zero. This means that the purely diffusive model [6] is available. Therefore, when the heat source is on, even if the data progress linearly, an ordinate at the origin related to the heat source of the equation [5] appeared.

The drawback is to find a processing to detect via the temperature field the diffusive behaviour [6] or not [5]. A way to distinguish is to study the coefficient $\rho_{i,j}^{F_t}$ of the correlation matrix defined as follow:

$$\rho_{i,j}^{F_t} = \frac{\sum_{F_t} \Delta T_{i,j}^k \delta T_{i,j}^k}{\sqrt{\sum_{F_t} \Delta T_{i,j}^{k\,2}} \sqrt{\sum_{F_t} \delta T_{i,j}^{k\,2}}} \qquad [7]$$

where F_t is a temporal window of length $F_t = [k, k+lt] with\ k \in [1, N-lt]$, with k the time step and lt the length of the temporal window.

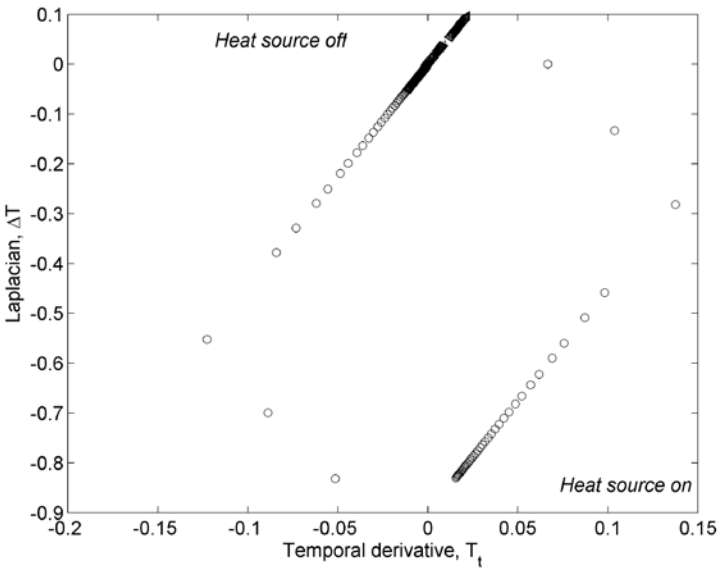

Figure 4. *Laplacian versus temporal derivative at every time step for the same three pixels located in the field of the Figure 3.*

If such correlation coefficient is near to 1, it is a proof that the purely diffusive model is available. When the heat source is off, the inverse thermal Fourier number related to the slope of the Figure 4 could be calculated with the formulation:

$$\frac{1}{Fo_{i,j}^{F_t}} = \frac{\sum_{F_t} \Delta T_{i,j}^k \delta T_{i,j}^k}{\sum_{F_t} \delta T_{i,j}^{k\,2}} = \frac{\rho_{i,j}^{F_t} \sqrt{\sum_{F_t} \Delta T_{i,j}^{k\,2}}}{\sqrt{\sum_{F_t} \delta T_{i,j}^{k\,2}}} \qquad [8]$$

Such a simple criterion can be applied for every temperature fields at each time step or with a time window. In the equation [8], the Laplacian term is taken as an observable. This is because the Laplacian is much more noised than the temporal derivative. If the model is purely diffusive, a perfect correlation ($\rho_{i,j}^{F_t} = 1$) between the Laplacian and the time derivative is obtained (Figure 5).

At the location of the heat source (Figure 5a), we observed a correlation equal to -1. This means that the simple diffusive model equation [6] is biased and that we cannot estimate a thermal diffusivity at this position and time of the process. In fact, the estimation of the thermal diffusivity will give a negative value corresponding to no physical meaning. Later (Figure 5b), when the heat source is off, we obtained a correlation equal to 1 at the same location.

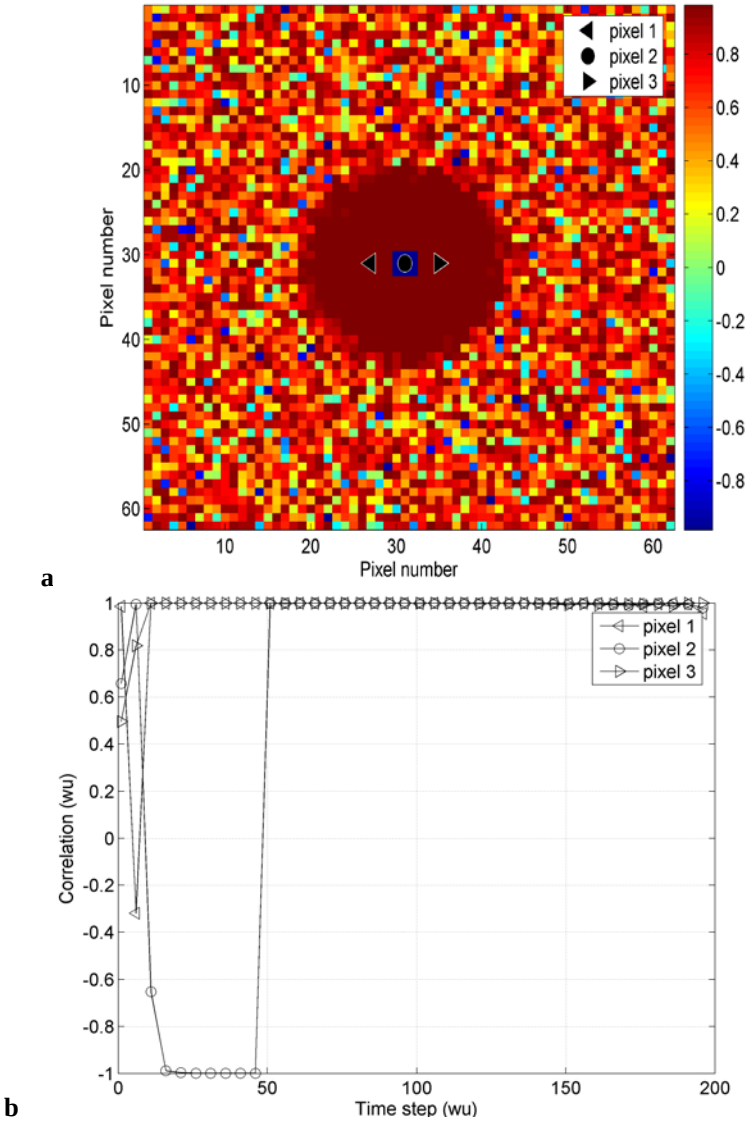

Figure 5. *Correlation matrix for Ft =2.* **a***) at time step Δt = 40, when many heat sources are on.* **b***) versus the entire time step for the three pixels located in the field of Figure 5a.*

This method allows estimating the diffusivity field (Figure 6) without any knowledge about the position in space and time of the source terms. *A fortiori*, it appears that a negative correlation allows detecting a bias in the simplified model equation [8], which is the proof of the presence of a source term.

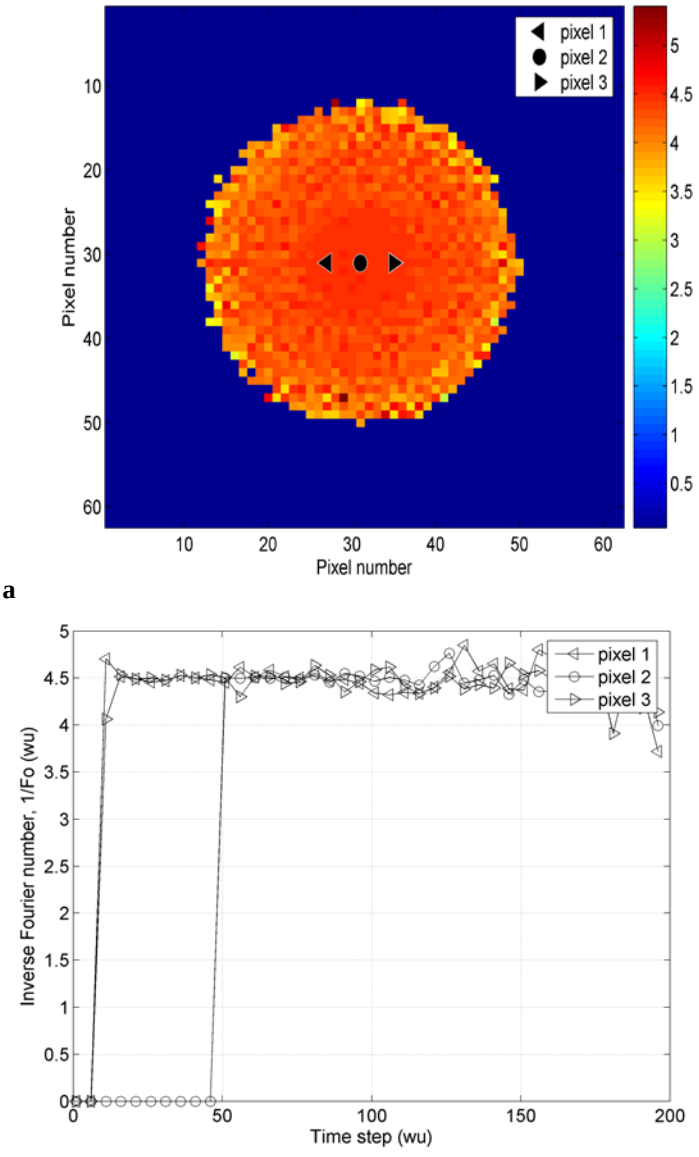

Figure 6. *Inverse Fourier number estimated:* **a***) field at the end of the processing* **b***) for the three pixels in the centre of the field versus the entire time step.*

The procedure for the estimation of the thermal diffusivity with equation [8] can be described. First we calculated the correlation equation [7] with a temporal window. When the value of the correlation was close to 1, we have estimated the thermal

diffusivity. Otherwise, the estimation was not performed and a zero value was affected. Under this consideration, at the end of the process we have obtained the field of global inverse Fourier number (Figure 6.a) calculated with the equation [9]:

$$\frac{1}{Fo_{i,j}^{est}} = \sum_{k=1}^{N-Ft} \frac{1}{Fo_{i,j}^{k}} . \left(\rho_{i,j}^{k} \to 1\right) \Bigg/ \sum_{k=1}^{N-Ft} \left(\rho_{i,j}^{k} \to 1\right) \qquad [9]$$

The results (Figure 6a) show that the inverse Fourier number field we have estimated is uniform on each pixel. We obtain an average value of 4.26 that can be use to calculate the thermal diffusivity $a = \Delta x^2 / (4.26\Delta t) = 1.05.10^{-6}$ m² s^{-1}. With an uncertainty lower than 5%, this is in good agreement with the matrix of thermal diffusivity we have generated. Further, the observation of the Figure 6b prove that for the pixels without source term (1 and 3), the thermal diffusivity is always estimated with a quasi-constant value. Otherwise, for the pixel located in the centre (2, where the source term is localised), the estimation of the thermal diffusivity is available just after that the source term is put off. Such kind of results is in good agreement with the correlation plotted (Figure 5b). The estimation of the inverse Fourier number is less accurate when the time step increases $\Delta t > 150$. This is due to the rapid decrease of the temperature with increasing time. A last signal processing step is then possible with the *a priori* knowledge of the diffusivity field, in order to estimate the instantaneous and local source field (Figure 7a), such as:

$$\Phi_{i,j}^{k} = \left(\delta T_{i,j}^{k} - Fo_{i,j}^{est} \Delta T_{i,j}^{k}\right) \qquad [10]$$

with $Fo_{i,j}^{est}$ the Fourier number estimated with the simple model [9]. In addition, the global heat source at the end of the process (Figure 7b) is estimated equation by a simple average versus time of the entire instantaneous estimated heat source.

The results (Figure 7a) show that the field of source term is well estimated in time and space with a value of $\Phi = 0.2004$°C. In fact the values are quite close to the field we have generated (Figure 2a). Finally, the source term estimated as a function of time is also in good agreement with the data (Figure 2b). Moreover, the heat source estimated on pixels 1 and 3 are equal to zero.

3. Results and discussion

3.1. *Experimental validation on homogeneous glass wafer*

An experimental validation is performed on a simple homogeneous media (glass wafer), with the same configurations as the numerical processing. As shown Figure 8, a glass wafer of 170 µm thickness and 5 cm diameter is black painted and deposit on an insulated foam block. A laser diode of 805 nm wavelength with a power ranging from 100 to 1000 mW is used to locally warm up the plate. With the optical configuration,

the diameter of the beam is close to 300 µm. The temporal evolution of the laser diode is the same as in the Figure 2b with a duration of 0.8 s. An IR CEDIP ORION camera, having an indium-antimony (InSb) sensor array of 256 x 256 pixels with an optimum wavelength between 2 µm and 5 µm and a IR microscope was used to measure the temperature field as a function of the time.

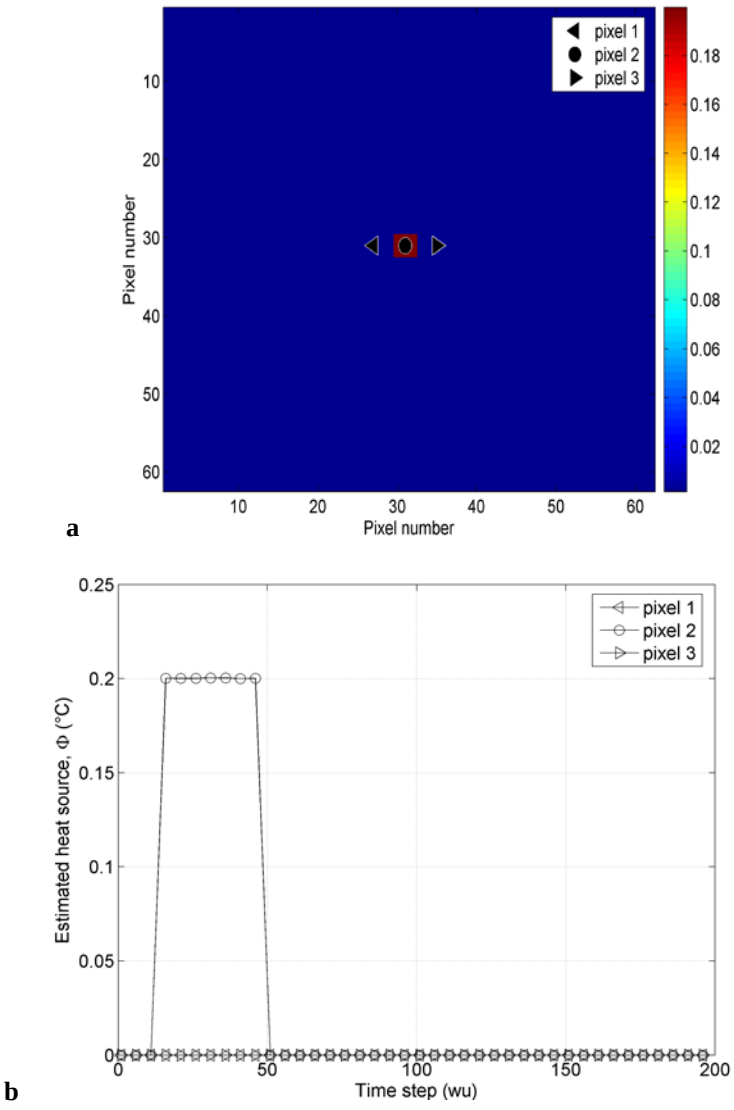

Figure 7. *Heat source estimated:* **a**) *field at the end of the processing* **b**) *for the three pixels in the centre of the field versus the entire time step.*

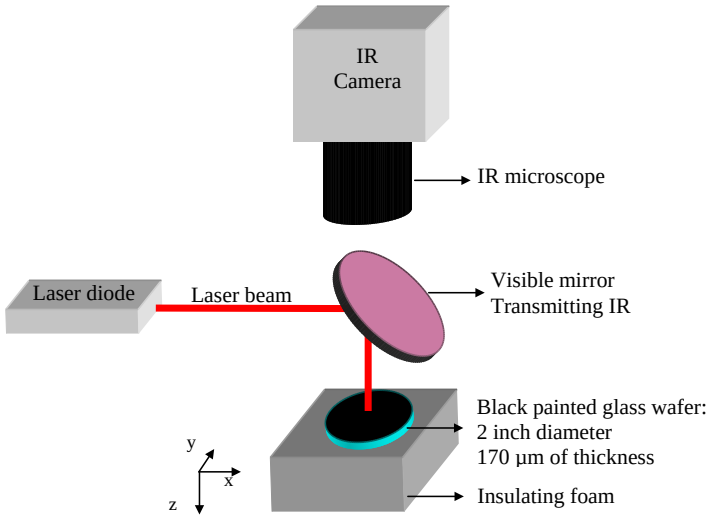
IR
Camera
IR microscope
Laser diode
Laser beam
Visible mirror
Transmitting IR
Black painted glass wafer:
2 inch diameter
170 µm of thickness
Insulating foam
y
x
z

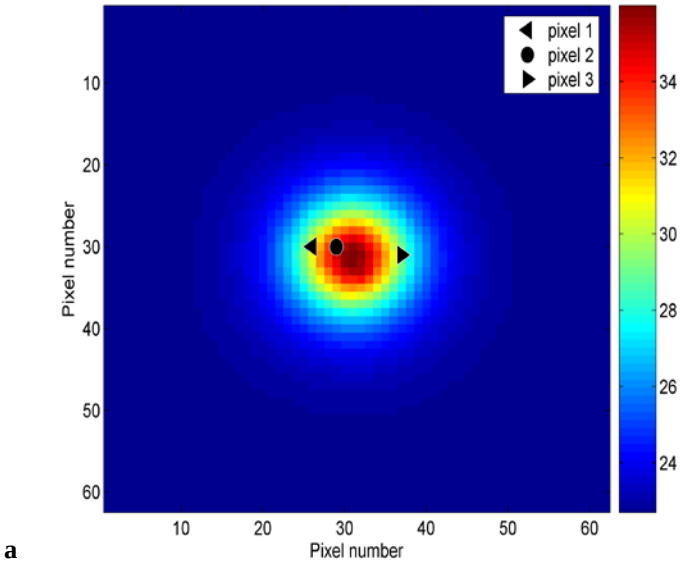

a

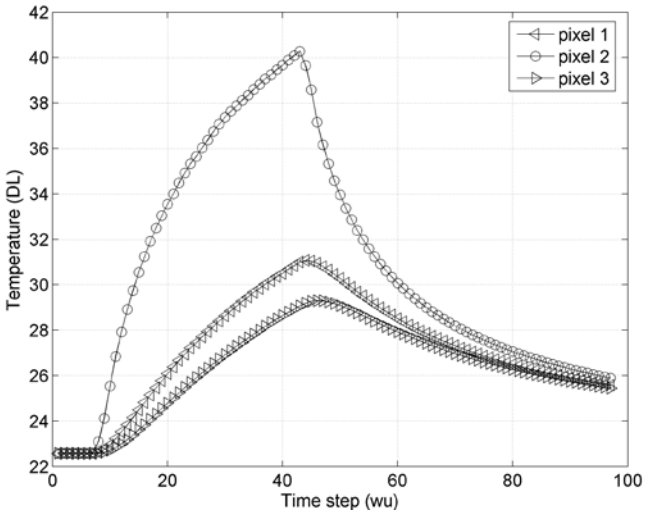

b

Figure 9. *Measured temperature in Digital Level for glass wafer:* **a***) spatial field representation at time step Δt = 49,* **b***) as function of time for three pixels in the centre of the field.*

with an average value of 1.623. With the value of the pixel size of 104 µm and the time step of 20 ms, this corresponds to a thermal diffusivity value of $3.33.10^{-7}$ m² s^{-1}. This value is lower than the literature one $3.4.10^{-7}$ m² s^{-1} (Holman 2002). Nevertheless, with a difference of less than 5 %, the uniformity is verified and the temporal estimation (Figure 11b) of the inverse Fourier number is assumed quite repetitive.

Finally, figure 12, the heat source (i.e. the laser diode power, spatial and temporal representation) is estimated by the relation [10] and the knowledge of the estimated inverse Fourier number (Figure 11a).

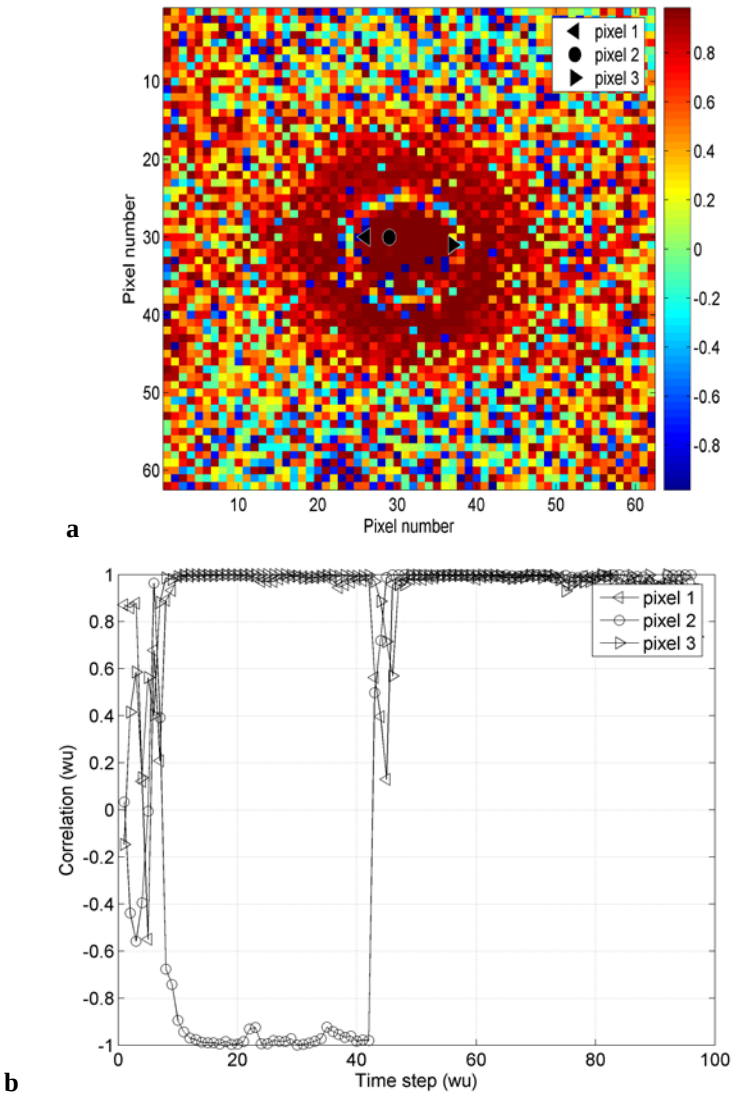

Figure 10. *Correlation matrix of the glass wafer for Ft =4.* **a***) at time step Δt = 49 when many heat sources are on.* **b**) *for the three pixels in the centre of the field versus the entire time step.*

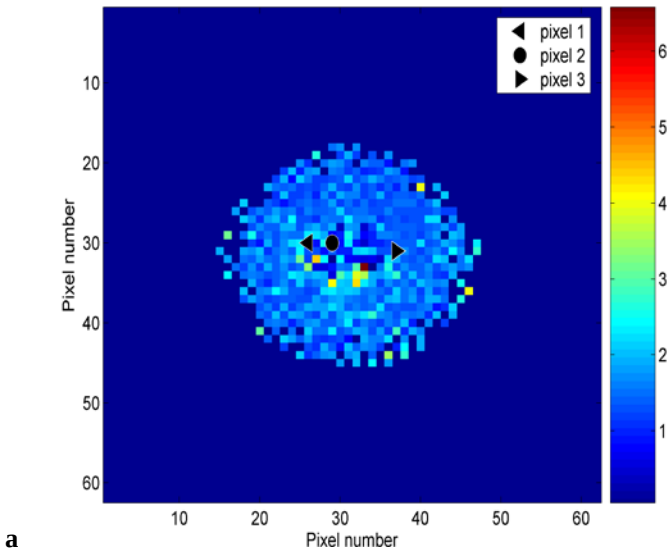

a

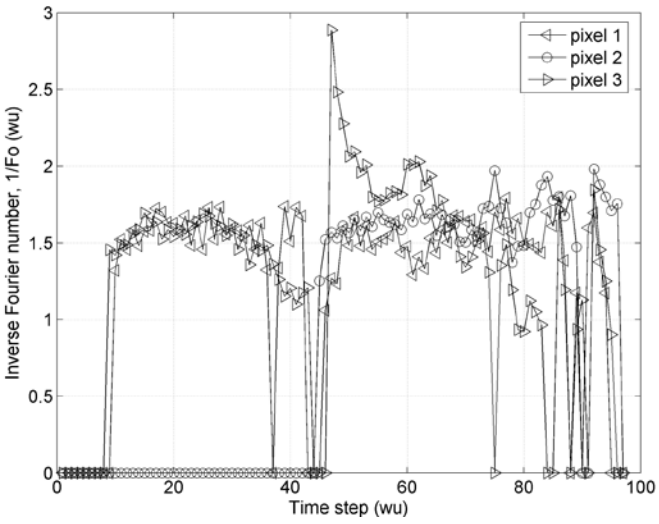

b

Figure 11. *Inverse Fourier number estimated for the glass wafer:* **a***) field at the end of the processing* **b***) for the 3 pixels in the centre of the field versus the entire time step.*

The averaged field of heat source (Figure 12a) is well localised in the centre of the field. The spatial average in x direction (Figure 12b) is in good agreement with a quasi-Gaussian energy repartition of the beam of the laser diode. Finally, the temporal evolution (Figure 12c) is in good agreement with the function of time we have imposed to the system (see Figure 2a) with an open state equal to 40 time steps (i.e. 0.8 s with Δt = 20 ms).

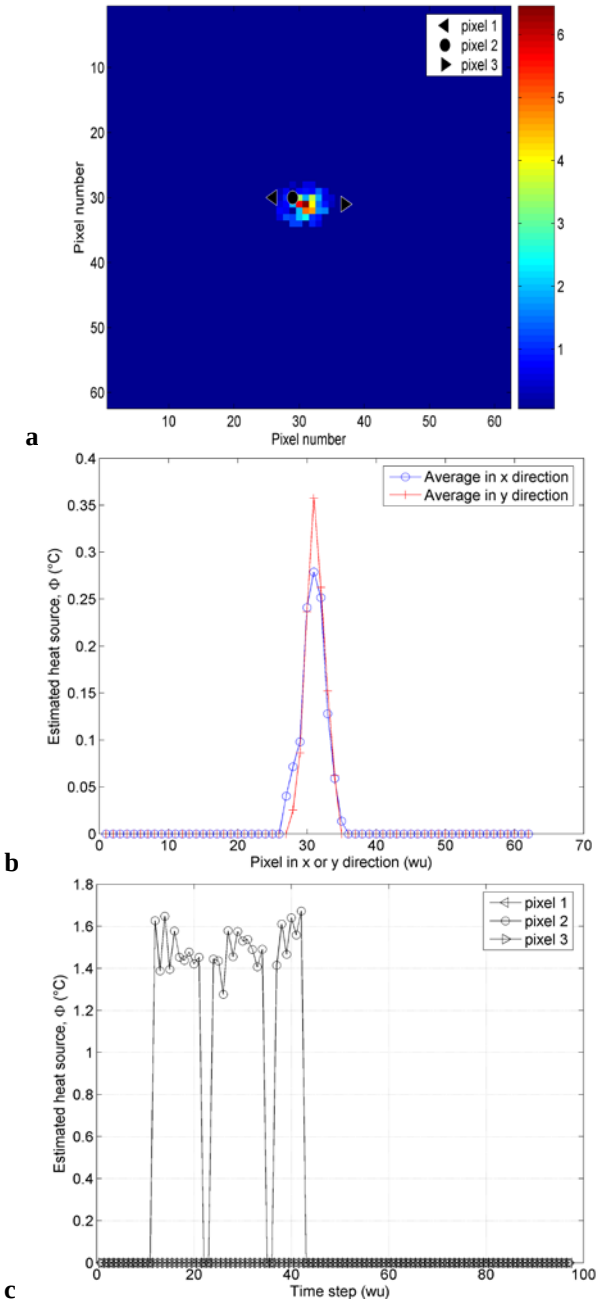

Figure 12. *Heat source estimated for the glass wafer:* **a***) field at the end of the processing* **b***) spatial average in x and y directions and* **c)** *for the three pixels in the centre of the field versus the entire time step.*

3.2. *Results and discussion on onionskin*

The processing method developed in section 2 is directly applied to the temperature field measured by Morikawa (Figure 13) with the experimental setup of the Figure 1, and parameters described in section 2.1.

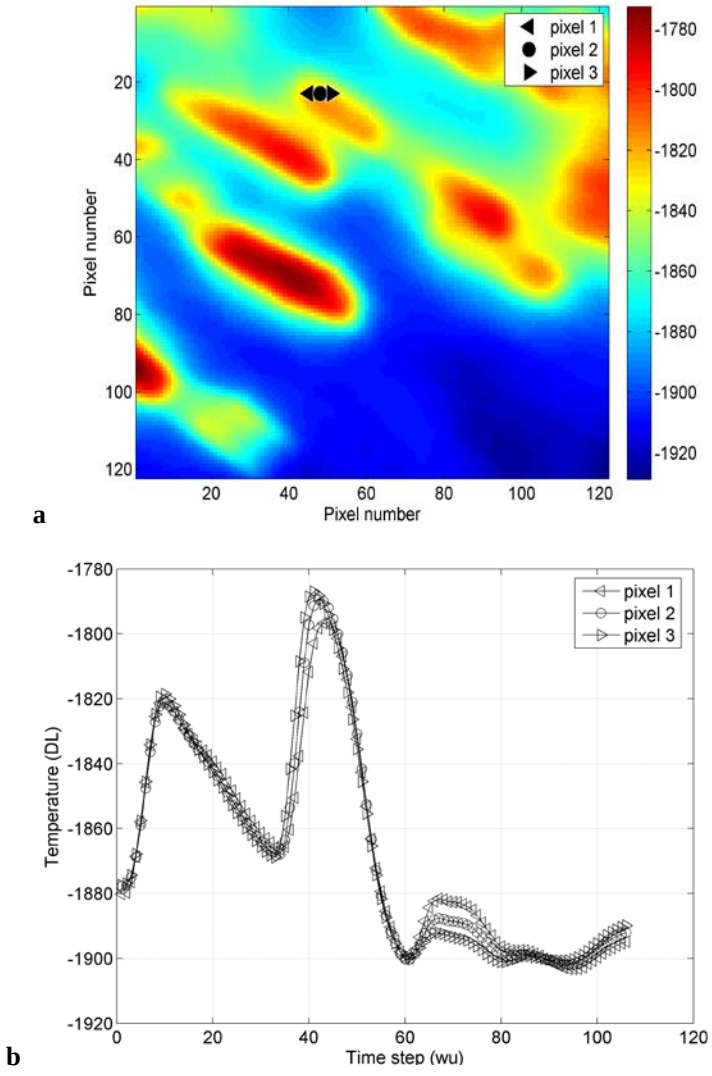

Figure 13. *Instantaneous temperature field in Digital Level obtained on onionskin during freezing process:* **a)** *at time step* $\Delta t = 40$, **b)** *for the three pixels in the centre of the field versus the entire time step.*

The first remark is that in the case of onion freezing, many cells have a phase change. These cause major difficulties with classical analysis. The other one is that for the pixels we have chosen the temperature variation is very similar for each phase change.

As described in the previous part (see section 2), the correlation matrix (Figure 14a) can be calculated for each window time (here $F_t = 4$).

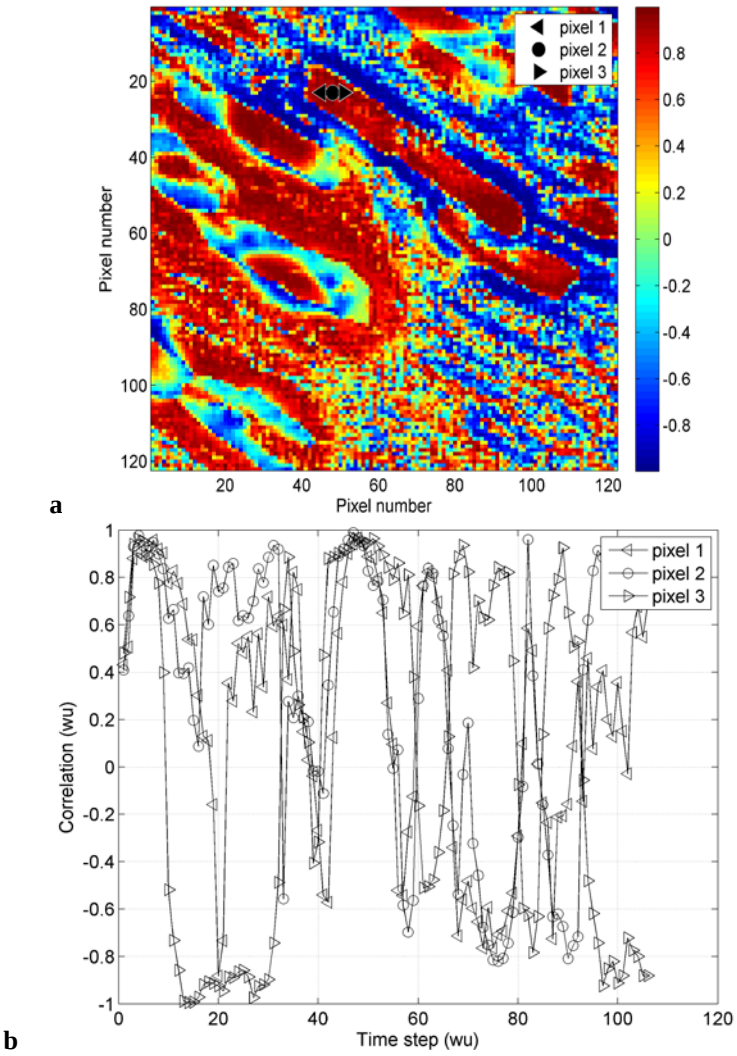

Figure 14. *Correlation matrix for F_t =4:* **a)** *at time step Δt = 40 when many heat source are on and* **b)** *for the three pixels in the centre of the field versus the entire time step.*

For the pixels 1, 2 and 3 chosen (Fig. 14a), the temporal variation of the correlation are shown Figure 14b. We clearly observe a variation of the correlation values from -1 to 1. This presupposed that many phase change occurred when ($\rho_{i,j}^{F_t} = -1$) and just after, when ($\rho_{i,j}^{F_t} = 1$), estimation of the thermal diffusivity could be performed.

With respect to the procedure, the total inverse Fourier field is estimated (Figure 15a) with the equation [9].

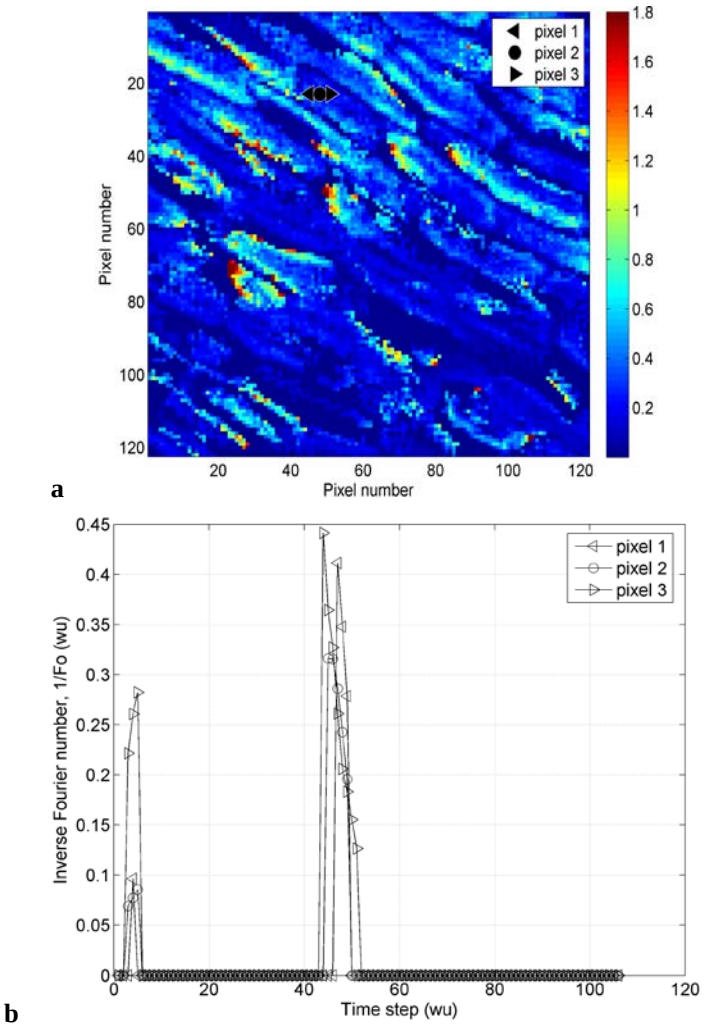

Figure 15. *Thermal diffusivity estimated:* **a)** *field at the end of the processing* **b)** *for the three pixels in the centre of the field versus the entire time step.*

The inverse Fourier number field allows us to distinguish the texture of the onion. We see that for many cells, the thermal diffusivity is higher in the surrounding of the cell, whereas in the centre of the cell the thermal diffusivity is lower and quasi homogeneous. Thus, there are many regions where the inverse Fourier number was not estimated. The thermal diffusivity is estimated versus time for the three pixels (1, 2 and 3) as a result from the succession of phase change. We observe that the inverse Fourier number increases. This means that the thermal diffusivity increases. This is consistent with the phase change of the onion cell from liquid water to solid ice.

With the knowledge of the thermal diffusivity fields, and with the equations [10], the total heat source field is then estimated. The results, (Figure 16b) are quite close to those observed for the thermal diffusivity. This confirms the fact that the phase change is preponderant and localised at the surrounding of the cell (figure 16a). Then, the source term versus time for the 3 pixels (figure 16c) is also interesting. It is shown that there is (in this case: space location) an exothermic phase change. The observation of the field of heat source (figure 16b) proves that the inner part of the cell is preserved from the phase change. In fact, it clearly appears parts where the heat source is null inside the cell. This means that the cell is living because no ice is inside the cell. With this processing tool, systematic study could be performed with different temperature range and rate in order to control ice propagation into the cell. By the application of two techniques, this one and classical biological one it will be interesting to match the position where the cells died or live.

The measurements performed on the onionskin are very interesting and seem to be in good agreement with the method we have developed. In fact, if we look at the correlation, thermal diffusivity and source term evolution versus time, it clearly appears that when the correlation is close to -1, the source term was estimated. This corresponds to an increase of the temperature. Whereas, after the source term was off, the estimation of the thermal diffusivity was possible and well identified by the value of the correlation close to 1 and a decrease of the temperature (associated to a relaxation).

Finally, the comparison with the previous work (Figure 17), proves the importance to take care of the diffusion process in the simultaneous estimation of the thermal diffusivity and source term. In fact, the temporal evolution of the source term estimated by only the time derivative gives results where the influence of the diffusion process and the phase change are correlated. For example, the negative values of the temporal derivative correspond to the part where the media relaxed (i.e. where the correlation is equal to 1). That means the location where the thermal diffusivity was estimable. The positive values of the temporal derivative give the part where the source term is on. However (figure 17a), the omission of the diffusion term (i.e. Laplacien) did not allow to well localize the source term (in comparison with the figure 16a).

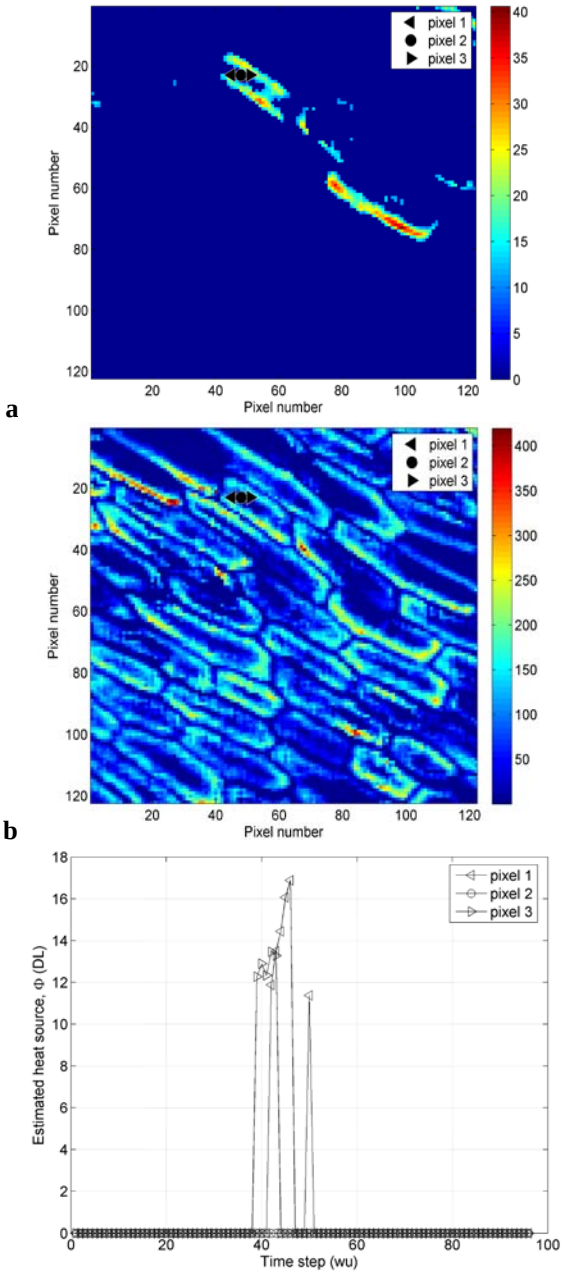

Figure 16. *Heat source estimated:* **a)** *instantaneous field at time step equal to 40* **b)** *field at the end of the processing* **c)** *for the three pixels in the centre of the field versus the entire time step.*

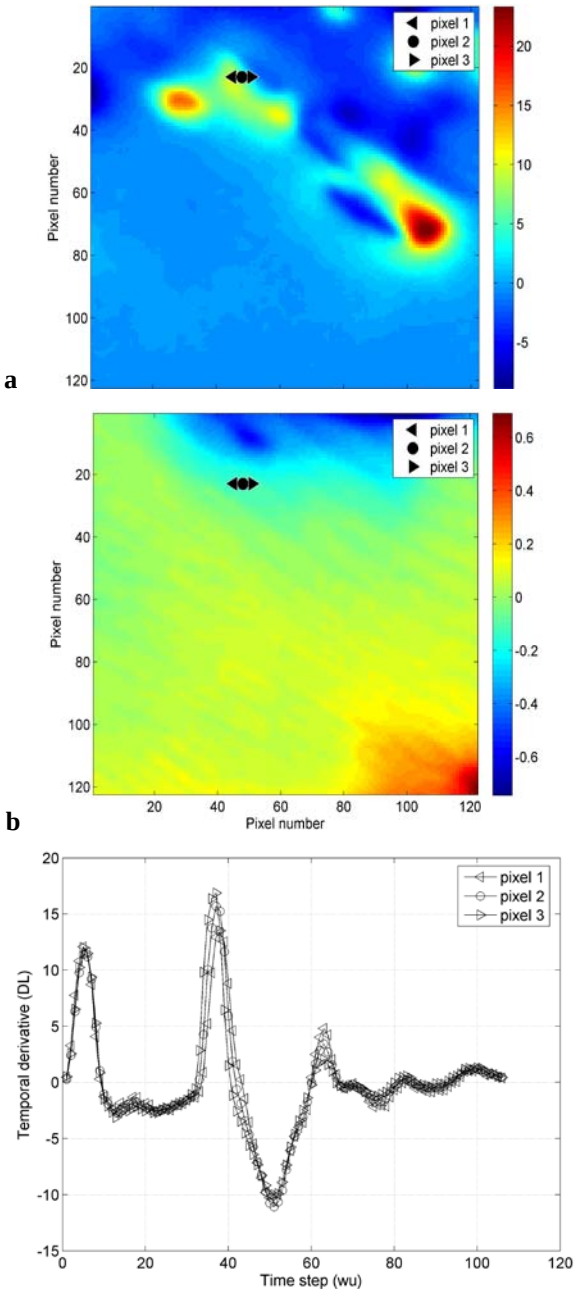

Figure 17. *Temporal derivative calculated (see Morikawa et al., 2006):* **a)** *instantaneous field at time step equal to 40* **b)** *field at the end of the processing* **c)** *for the three pixels in the centre of the field versus the entire time step.*

4. Conclusion and outlooks

Such results highlight interesting possibilities for the localization of source terms during cryopreservation processes from infrared images sequences. The diffusion analysis clearly demonstrates that the phase change does generally not occur at the centre of the cell but near the membrane. The diffusivity mapping is heterogeneous and corresponds to the structure of the cells. This proves the importance of the diffusion process in such system. In fact, to avoid damaging the tissue it is important to well know the thermal diffusivity of the media.

The processing method allows distinguishing, clearly and easily, the parts where the heat source are localized and the parts where the estimation of the thermal diffusivity is possible. The advantage of such processing is to avoid a previous calibration of the diffusivity of the system. It is then a way to implement a simultaneous two parameters estimation without a two parameters least square approach. Therefore, it is very important to notice that such processing use directly the source term of the phase change as a thermal excitation for the estimation of the thermal diffusivity. For that, the correlation coefficient is necessary to localize in time and space the pixels where a purely diffusive model is available. From this simple model, the global field of thermal diffusivity is estimated allowing the calculation of the heat source field.

The perspective of this work is to use such method in order to compare the effects of cryoprotective agents in order to avoid cell damage.

5. References

Diller K.R., “Intracellular freezing: effect of extra-cellular supercooling”, *Cryobiology*, Vol. 12, No. 5, pp. 480-485, 1975.

Hashimoto T., Morikawa J., “Two-dimensional microscale thermal analysis of freezing of onionskin cells by high-speed infrared focal plane arrays”, *Jpn. J. Appl. Phys. Part 2*, Vol. 42, No. 6B, pp. L706-L708, 2003.

Holman J.P., *Heat Transfer*, 9th Ed., McGraw-Hill, 2002.

Levin R.L., “The freezing of finite domain aqueous solutions: solute redistribution”, *Int. J. Heat Mass Transfer*, Vol. 24, No. 9, pp. 1443-1455, 1981.

Mazur P., “Kinetics of water loss from cells at subzero temperatures and the likelihood of intracellular freezing”, *J. Gen. Physiol*, Vol. 47, No. 2, pp. 347-369, 1963.

Morikawa J., Hashimoto T., Eto T., “Two-dimensional thermal analysis of organic materials by IR thermography”, *QIRT 2006 Conference*, Padova, Italy, 28-30 June 2006. – Loadable on *QIRT* Open Archives, paper QIRT 2006-036 (http://qirt.gel.ulaval.ca/archives/qirt2006/papers/036.pdf).

Toner M., Cravalho E.G., Karel M., “Thermodynamics and kinetics of intracellular ice formation during freezing of biological cells”, *J. Appl. Phys*, Vol. 67, No. 3, pp. 1582-1593, 1990.